The Astronomical Journal, 123:2574–2582, 2002 May

DETECTION OF THE WINDS FROM THE EXCITING SOURCES OF SHELL H II REGIONS IN NGC 6334

Patricia Carral
Departamento de Astronomía, Universidad de Guanajuato, Apdo. Postal 144, 36000 Guanajuato, Gto., Mexico; patricia@astro.ugto.mx

Stan E. Kurtz and Luis F. Rodríguez
Instituto de Astronomía, Universidad Nacional Autónoma de México, Apdo. Postal 3-72, 58090 Morelia, Mich. México; s.kurtz@astrosmo.unam.mx, l.rodriguez@astrosmo.unam.mx

Karl Menten
Max-Planck-Institut für Radioastronomie, Auf dem Hügel 69, D-53121 Bonn, Germany

Jorge Cantó
Instituto de Astronomía, Universidad Nacional Autónoma de México, Apdo. Postal 70-264, 04510 México D.F., Mexico

and

Roberto Arceo
Escuela de Ciencias Físico-Matemáticas, Universidad Michoacana de San Nicolás de Hidalgo, 58040 Morelia, Mich., Mexico
Received 2001 November 7; accepted 2002 January 17

ABSTRACT

We present results of high-sensitivity, high-resolution, multifrequency VLA observations toward the star-forming complex NGC 6334. We find that the H II region NGC 6334E, previously described as spherical, has a shell-like morphology. An additional shell-like radio source, G351.02+0.65, is mapped at 330 MHz. Four radio sources in the NGC 6334 complex present shell-like morphology; their diameters vary from 0.12 to 3.5 pc. Compact radio sources are detected at the center of the shells of NGC 6334E and NGC 6334A. These compact sources are believed to be associated with the exciting stars and are probably tracing ionized stellar winds. This is the first time for any H II region that both the shell and the central object are detected simultaneously in the radio. Two compact radio sources are detected toward the NGC 6334I(N) molecular core. One of them lies within 0.″3 of the position of a bright Class II methanol maser, suggesting that the radio source is associated with a young embedded massive star. This is the first detection of a radio continuum source in the NGC 6334I(N) region.

Key words: H II regions — radio continuum — stars: early-type — stars: formation

1. INTRODUCTION

The massive star forming region NGC 6334 has been the subject of numerous studies at radio and infrared wavelengths. It has an associated molecular cloud which is elongated (size $\sim 45'$) and oriented parallel to the Galactic plane (Dickel, Dickel, & Wilson 1977). The cloud, located at a distance of 1.7 kpc (Neckel 1978), contains several luminous centers of active star formation which seem to be at different evolutionary stages (McBreen et al. 1979; Moran & Rodríguez 1980; Rodríguez, Cantó, & Moran 1982; hereafter RCM). The 69 μm map of McBreen et al. (1979) shows five centers of active star formation. The northernmost of these, named NGC 6334I, is associated with the ultracompact H II region NGC 6334F (RCM), as well as with maser emission from OH, H_2O, CH_3OH, and $NH_3(3,3)$ (Gaume & Mutel 1987; Forster & Caswell 1989; Menten & Bartla 1989; Kraemer & Jackson 1995; Moran & Rodríguez 1980; Norris et al. 1993), an energetic bipolar outflow (Bachiller & Cernicharo 1990; Davis & Eisloeffel 1995; Persi et al. 1996; McCutcheon et al. 2000), and a star cluster (Tapia, Persi, & Roth 1996; hereafter TPR). Continuum observations and the detection of a rich molecular spectrum indicate that NGC 6334I has an associated compact hot molecular core of a few hundred solar masses (Kuiper et al. 1995; Gezari 1982; Cheung et al. 1978; Forster et al. 1987; Menten & Bartla 1989; Mangum & Wootten 1993; McCutcheon et al. 2000; Sandell 2000). NGC 6334I is believed to be one of the youngest star forming regions in the complex.

The region is a complicated one, and unfortunately this is reflected in the nomenclature of the sources. In the scheme that has evolved, letter designations (NGC 6334 A–F) correspond to centimeter radio sources (RCM), while roman numeral designations (NGC 6334 I–VI) are used for millimeter and infrared sources. Regrettably, the roman numerals of Cheung et al. (1978) at 1 mm and those of McBreen et al. (1979) at 69 μm do not directly correspond to one another. We adopt the convention of Gezari (1982), in which NGC 6334I is source I in the nomenclature of McBreen et al., while NGC 6334I(N)—about 2′ north of source I—refers to source I in Cheung et al.'s notation. The latter source was not detected by McBreen et al., but Cheung et al. found it to be the strongest 1 mm peak in the NGC 6334 complex and to be lacking any infrared or radio counterpart. A large column density of $\sim 10^{24}$ cm^{-2} was derived for this region, and Moran & Rodríguez (1980) detected a water maser. Gezari (1982) derived an infrared luminosity of 7000 $L_\odot$ and suggested that this cool source ($T \simeq 20$ K) required the presence of one or more embedded B stars. Loughran et al. (1986) proposed a bolometric luminosity of 56,000 $L_\odot$. Despite this large value, suggestive of an O9 ZAMS star, a reanalysis of the 6 cm data of RCM shows no continuum source in the region at a 4 σ level of 3 mJy. Recently, several other star formation indicators have been detected in NGC 6334I(N): Class I (Kogan & Slysh 1998) and Class II (Caswell et al. 1993; Norris et al. 1993; Walsh et al. 1998; Caswell 1997) methanol masers, a molecular outflow (Megeath & Tieftrunk 1999), a bright molecular core (Kuiper et al. 1995, Kraemer & Jackson 1999, McCutcheon et al. 2000), and submillimeter sources (Sandell 2000). The high-resolution submillimeter continuum observations by Sandell (2000) resolve Gezari's cold source I(N) into a compact (FWHM $\sim 10''$, 82 mpc) dust source with a luminosity of 1.9×10^3 $L_\odot$, which is embedded in a dense cloud core with a total luminosity of about 1.7×10^4 $L_\odot$.

A $\sim 20''$ diameter H II region lies between NGC 6334I and NGC 6334I(N), slightly offset to the west (RCM). Named NGC 6334E, this H II region requires the equivalent of an O7.5 ZAMS star to provide the photons that maintain the ionization of the gas. It appears to be associated with little dust as seen in millimeter and submillimeter maps (Sandell 2000; McCutcheon et al. 2000). Near-infrared observations of the source show extended emission at K band with an angular size similar to that of the H II region (TPR). TPR also identified a red object coincident with the peak position of NGC 6334E (their source 161).

Another H II region, NGC 6334A, first reported by RCM, coincides with peak IV of McBreen et al. (1979) and requires an O7.5 ZAMS star to ionize the surrounding gas. It has a shell-like radio structure with extended bipolar plumes that extend north-south (Rodríguez, Cantó, & Moran 1988). Near-infrared observations show diffuse bipolar emission nearly coincident with the radio lobes (Harvey, Hyland, & Straw 1987; Harvey & Gatley 1983). A water maser and an ionized outflow have been detected near the source (De Pree et al. 1995), as well as an elongated molecular structure oriented in the east-west direction (Moran & Rodríguez 1980; Kraemer et al. 1997)

In this article we report high-sensitivity, high-resolution observations of the NGC 6334 H II complex, including the ultracompact H II region NGC 6334F. In addition we reanalyzed radio data for NGC 6334A, NGC 6334E, and G351.02+0.65, part of which has been previously reported (RCM, Rodríguez et al. 1988, Moran et al. 1990, Carral et al. 1997). The goals of the observations were to search NGC 6334A and NGC 6334E for compact sources, to obtain a high-quality 7 mm image of NGC 6334F, and to provide a high-sensitivity 3.5 cm map of NGC 6334I(N) and the surrounding area to search for compact radio continuum sources which could trace young stellar objects. In § 2 we describe the observations, and in § 3 we discuss the results.

2. OBSERVATIONS

All observations reported here were made using the Very Large Array (VLA) of the National Radio Astronomy Observatory (NRAO).[1] The data were edited, calibrated, and imaged using the software package Astronomical Image Processing System (AIPS) of NRAO. The observations are summarized in Table 1. Several of the observations were made with B1950.0 coordinates, but, for uniformity, in all cases we list J2000.0 pointing centers and calibrator names.

The northeast part of the NGC 6334 complex was observed at 3.5 cm on 1995 August 11 in the A configuration, with pointing center $\alpha(2000) = 17^{\rm h}20^{\rm m}53\overset{\rm s}{.}4$; $\delta(2000) = -35°46'25''$. The 4IF spectral line mode was used with eight channels in a bandwidth of 25 MHz. The on-source integration time was about 3.8 hr. The absolute flux calibrator was 3C286, and NRAO 530 (1733−130) was used to calculate the antenna gains. The data were self-calibrated in phase and amplitude.

The NGC 6334F region was observed at 7 and 13 mm in the D configuration on 1995 February 20 and 1999 April 20. The 1995 data were reported by Carral et al. (1997). Observations were also made at 13 mm and 2 cm on 1997 January 31 in the BnA configuration. For all these observations a 100 MHz bandwidth was employed, centered at the nominal VLA frequencies of 43.34, 22.46, and 14.94 GHz. The absolute flux calibrator was 3C286 in all cases, while 1720−358, 1700−261, and 1626−298 were used as gain calibrators.

Multiepoch data sets at 7 and 13 mm were combined, and at all wavebands the data were self-calibrated. Observing times were typically 1–2 hr at each wavelength. In 1997 both wavelengths were observed with the full array, while in 1995 and 1999 observations were made simultaneously with the array divided between the 7 and 13 mm bands. In addition, we reanalyzed the 6 cm data presented by RCM and the 3.5 cm data obtained in the BnA configuration on 1997 February 2. Data at 90 cm (330 MHz) obtained with the VLA in the BnA configuration on 1989 March 5 were also analyzed.

3. RESULTS AND DISCUSSION

3.1. *NGC 6334F*

The fluxes obtained for the ultracompact H II region NGC 6334F at 6.0, 3.5, 2, 1.3, and 0.7 cm are presented in Table 2. Our new map at 7 mm (see Fig. 1) does not confirm the detection of emission to the west of the cometary arc reported by Carral et al. (1997). We suspect that the emission they report was not real but rather appeared as an artifact of the data reduction and the limited (u, v) coverage of the 1995 data.

3.2. *NGC 6334I(N)*

To search for faint, compact radio sources, we made a 3.5 cm map with the task IMAGR and the ROBUST parameter set to zero, using only visibilities with a (u, v) distance larger than 150 kλ. This procedure suppresses the emission from the nearby extended sources NGC 6334F and NGC 6334E that would obliterate faint, compact sources. In a $1' \times 1'$ region centered on the peak submillimeter position of Sandell (2000), $\alpha(2000) = 17^{\rm h}20^{\rm m}55\overset{\rm s}{.}2$; $\delta(2000) = -35°45'08''$, we detect only two sources above a 5 σ level of 0.31 mJy. One of these (source 1) is located at $\alpha(2000) = 17^{\rm h}20^{\rm m}55\overset{\rm s}{.}20$; $\delta(2000) = -35°44'42\overset{''}{.}6$, with a flux density of 0.41 ± 0.06 mJy and is not associated with previously known objects. The other, however (source 2), located at $\alpha(2000) = 17^{\rm h}20^{\rm m}54\overset{\rm s}{.}63$; $\delta(2000) = -35°45'08\overset{''}{.}5$ with a flux density of 0.34 ± 0.06 mJy, coincides within $0\overset{''}{.}3$ with the bright Class II methanol maser 351.445+0.660 (Caswell 1997), as shown in Figure 2. The error in the radio positions is $0\overset{''}{.}1$. This is the first detection of a radio continuum source in the NGC 6334I(N) region. For a distance of 1.7 kpc and assuming that the emission is optically thin free-free, we find that a late-B2 ZAMS star with luminosity of $\sim 10^3$ $L_\odot$

[1] NRAO is operated by Associated Universities, Inc., under cooperative agreement with the National Science Foundation.

TABLE 1

Summary of Observations

Date	VLA Configuration	λ (cm)	Pointing Center α, δ	Phase Calibrator	Flux Density (Jy)
1980 Apr 15.......	A/B	6.0	17 20 56.12, −35 46 12.2	1700−261	0.489 ± 0.001
1989 Mar 5........	BnA	90	17 20 21.79, −35 52 48.7	1701−299	6.39 ± 0.09
1995 Feb 20.......	D	0.7	17 20 53.44, −35 47 02.0	1700−261	1.64 ± 0.06
	D	1.3	17 20 53.44, −35 47 02.0	1700−261	2.00 ± 0.06
1995 Aug 11	A	3.5	17 20 53.40, −35 46 25.0	1733−130	7.6 ± 0.2
1997 Jan 31	BnA	2.0	17 20 53.44, −35 47 02.0	1626−298	2.77 ± 0.04
	BnA	1.3	17 20 53.44, −35 47 02.0	1626−298	2.67 ± 0.01
1997 Feb 2.........	BnA	3.5	17 20 21.79, −35 52 48.5	1733−130	11.68 ± 0.01
1999 Apr 20.......	D	0.7	17 20 54.14, −35 47 02.4	1720−358	0.69 ± 0.04
	D	1.3	17 20 54.14, −35 47 02.4	1700−261	0.48 ± 0.02

Note.—Units of right ascension are hours, minutes, and seconds, and units of declination are degrees, arcminutes, and arcseconds (J2000.0).

could provide the photons required to maintain the gas ionization.

Source 2 may also be associated with the I(N) submillimeter source detected by Sandell (2000) although it appears offset by 7″ from the submillimeter peak. The offset, however, could be less given the uncertainty in Sandell's position of a few arcseconds (see § 2.2 of Sandell 2000). Megeath & Tieftrunk (1999) detected an SiO outflow centered on the submillimeter compact core (see also McCutcheon et al. 2000). From the outflow parameters, Megeath & Tieftrunk suggest that a protostar with a luminosity of about $10^3\ L_\odot$ is generating the outflow. Hence, a star generating the radio continuum emission together with a protostar generating the outflow could provide the bolometric luminosity of $1.9 \times 10^3\ L_\odot$ estimated by Sandell (2000) for the compact core. However, the total luminosity of the I(N) region is $\sim 1.7 \times 10^4\ L_\odot$, so a cluster of embedded, lower mass stars seems to be required. Using the diagram of Carral et al. (1999) for the luminosity and ionizing photon rate expected for a star cluster (see their Fig. 3) we see that for NGC 6334I(N), a cluster of stars with an upper mass cutoff corresponding to a late-B2 star and which follows a Miller-Scalo IMF (Miller & Scalo 1979), cannot explain the total luminosity estimated for NGC 6334I(N). There seems to be an excess of bolometric luminosity for the amount of free-free radiation present. As discussed by Carral et al. for other objects, a possible explanation for this apparent lack of ionizing photons could be that the radio continuum emission detected is not generated in an H II region, but rather in a thermal jet. Such a jet would produce detectable, partially optically thick centimeter continuum emission but with a flux density 1 or 2 orders of magnitude below that expected from an optically thin H II region ionized by a ZAMS star with the observed luminosity. Another possibility is that we underestimate the ionizing photon rate, either because the radio continuum emission is optically thick or because dust is effectively competing with the gas for ionizing photons. An estimate of the spectral index of the radio source is required to further investigate these possibilities.

3.3. *Sources with Shell-like Morphology in NGC 6334*

Of the four radio sources we imaged, three of them, NGC 6334A, NGC 6334E, and G351.02+0.65, have a shell-like morphology. Another source in the NGC 6334 complex, G351.20+0.70, which we do not discuss, was also found to have a shell-like morphology (Jackson & Kraemer 1999). In two of these regions, NGC 6334A and NGC 6334E, we detected associated compact radio sources at the center of the shells. Various source parameters are summarized in Table 3. Next we describe the individual regions and in § 3.4 we discuss our general results.

3.3.1. *NGC 6334E*

A natural-weighted 3.5 cm map of the NGC 6334E region is shown in Figure 3. This region was originally classified as spherical by RCM. Our map, however, shows that a shell-like classification is more appropriate. The VLA cannot detect structures much larger than the angular resolution of a given observation. For the A, B, and C configurations used, the largest angular scales detectable by the VLA are about 30 times larger than the angular resolution. For the D configuration, this factor is about 20. Since the NGC 6334E source was observed in the A configuration, the emission on spatial scales larger than about 7″ is not properly imaged. The total flux estimates, therefore, are unreliable. The shell was detected also in our 1.3 cm map, but it falls near the edge of the primary beam, making the flux determination uncertain. At 6 cm this H II region has a total flux density of ∼12 Jy and requires an O7.5 ZAMS star to maintain its ionization (RCM). The map at 3.5 cm shows that the shell has surface brightness variations along the circumference as well as two gaps, one to the northwest and one to the southeast. The shell diameter is ∼30″ or 0.25 pc at a distance of

TABLE 2

Continuum Flux Densities of NGC 6334F

Parameter	Value				
λ (cm).........	6.0	3.5	2.0	1.3	0.7
S_ν (Jy)	3.0 ± 0.3	2.9 ± 0.3	2.8 ± 0.2	2.8 ± 0.3	2.0 ± 0.3

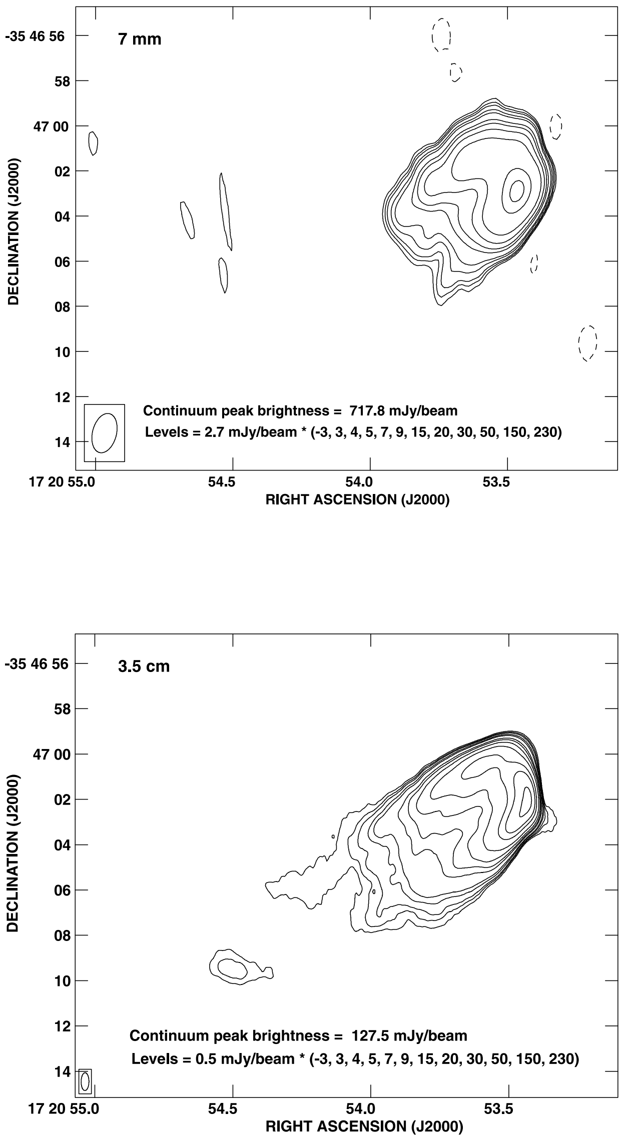

FIG. 1.—*Top*: High-sensitivity 7 mm continuum image of NGC 6334F. Contour levels are in multiples of the rms noise of 2.7 mJy beam^{-1}. No evidence is seen for the " bulge " on the western side of the cometary arc as reported by Carral et al. 1997. Also undetected is the clump of emission to the east of the region, as seen in the 3.5 cm map below. *Bottom*: High-sensitivity 3.5 cm continuum image of NGC 6334F. Contour levels are in multiples of the rms noise of 0.5 mJy beam^{-1}.

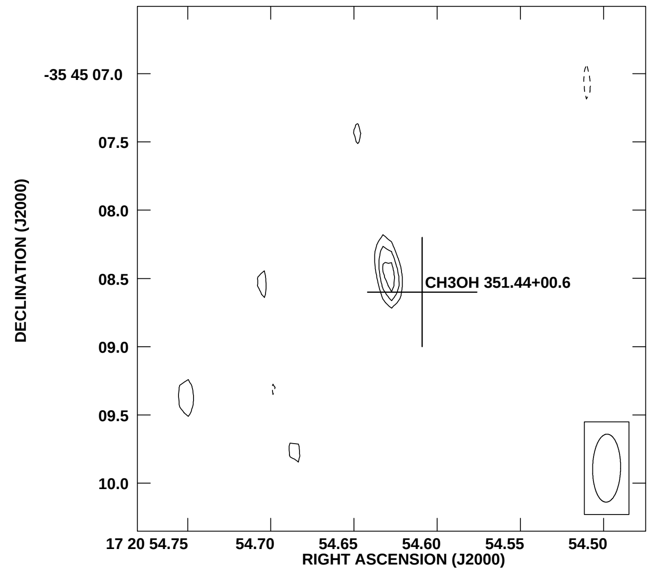

FIG. 2.—Contour map of the 3.5 cm source apparently associated with the Class II methanol maser 351.44+0.60 (Caswell et al. 1993). Contours are −3, 3, 4, and 5 × 61 μJy beam^{-1}, the rms noise of the map. The cross marks the location and positional uncertainty of the methanol maser, taken from Caswell (1997).

1.7 kpc, and the thickness is roughly 4″, or 0.03 pc. Equating the number of ionizing photons produced by an O7.5 star to the number of recombinations in the shell, we estimate the density at $n_e \sim 7 \times 10^3$ cm^{-3} and the mass of ionized gas in the shell at $M_{\rm H\,II} \sim 1\ M_\odot$, assuming spherical symmetry.

Our 3.5 cm map reveals a compact source at the center of the H II region (see Fig. 3). This source is unresolved ($\lesssim$0$''\!.$3, 510 AU) and has a flux density of 1.3 ± 0.1 mJy. This flux density was measured from a map made by removing short spacings below 100 kλ (equivalent to suppressing structures with angular size larger than about 2″) and using uniform weight. At 1.3 cm we also detect the compact source and, in a map including all the data (with a u, v range from 2 to 94 kλ), we measure a flux density of 3.5 ± 1.0 mJy. From the reanalyzed 6 cm data of RCM, we set a 4 σ upper limit of 2.4 mJy at this frequency. The compact radio source is located, with an estimated error of 0$''\!.$1, at $\alpha(2000) = 17^{\rm h}20^{\rm m}50\overset{\rm s}{.}9$; $\delta(2000) = -35°46'4''\!.8$, less than 0$''\!.$5 from the red source TPR 161 as measured by 2MASS. The infrared and radio sources are probably associated to the same object, and its location, as well as its infrared colors, strongly suggest that

TABLE 3

PARAMETERS OF REGIONS WITH SHELL MORPHOLOGY IN NGC 6334

Region	Shell 6 cm Flux Density (Jy)	Diameter[a] (pc)	Thickness[a] (pc)	Central Source 3.5 cm Flux Density (mJy)
NGC 6334 A	~10[b]	0.12	0.016	6.1 ± 0.9
NGC 6334 E	~12[b]	0.25	0.03	1.3 ± 0.1
G351.20+0.70	4[c]	1.1[d]	0.2[d]	. . .
G351.02+0.65	$\gtrsim$4.5	3.5	0.4	. . .

[a] Rough estimates from the maps.
[b] From RCM.
[c] From Moran et al. 1990.
[d] From Fig. 1 of Jackson & Kraemer 1999.

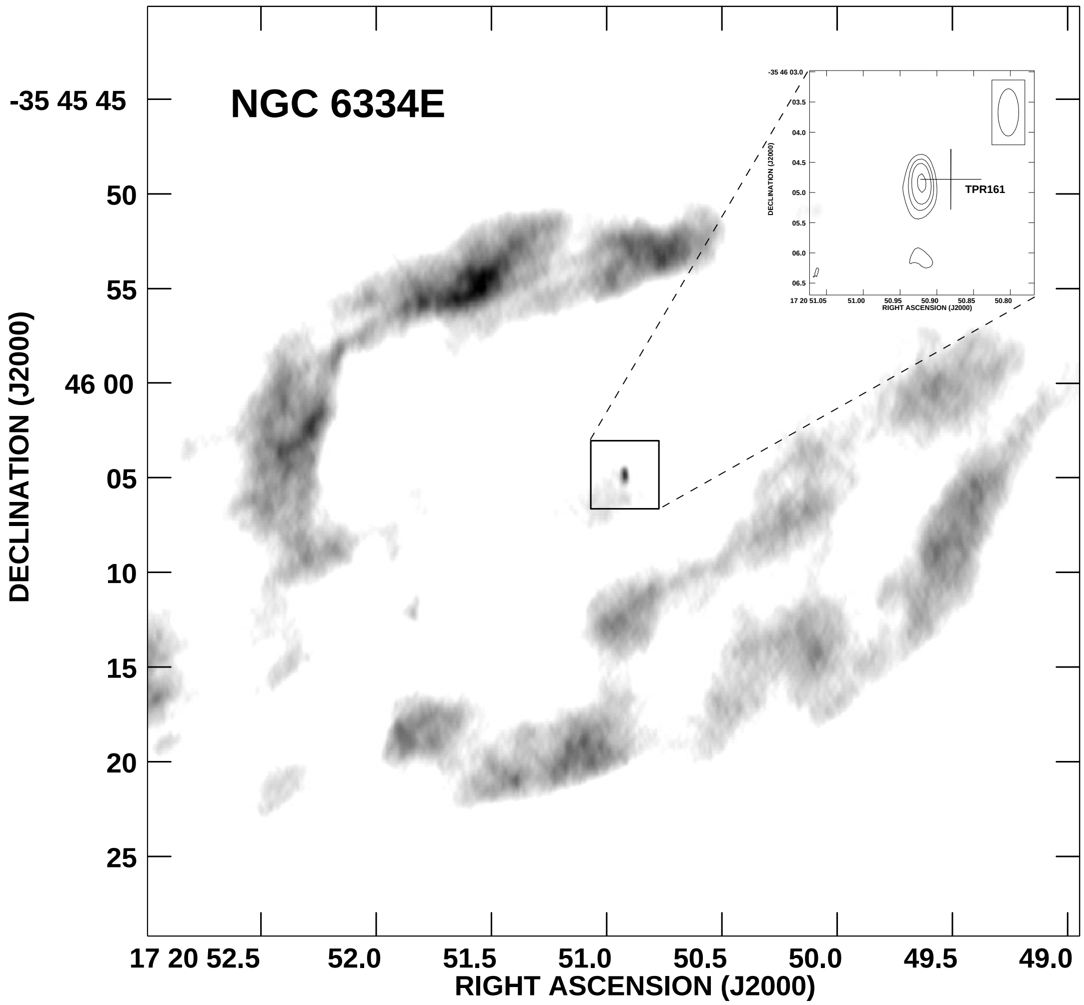

FIG. 3.—Gray-scale map at 3.5 cm of the shell-like H II region NGC 6334E, made with natural weighting. The emission shown is that above 0.6 mJy beam^{-1}, with a peak value of 2.1 mJy beam^{-1}. Contours (*inset*) are -4, 4, 5, 6, and 8 $\times$ 0.2 mJy beam^{-1}. The cross marks the position of the near infrared source, TPR 161, taken from 2MASS. The half-power contour of the beam ($0\farcs78 \times 0\farcs34$; P.A. $= -1°$) is shown in the top right corner.

it is the star ionizing NGC 6334E (see also TPR). From the 3.5 and 1.3 cm flux densities we estimate a spectral index $\alpha = 1.0 \pm 0.7$. Such an index is compatible, within the uncertainty, with thermal emission generated in an ionized stellar envelope with a density gradient $n_e \propto r^{-2}$, where r is the distance to the star. A stellar wind can result in this density profile and therefore produce the observed spectral index (Panagia & Felli 1975). Multifrequency VLA observations should be made, however, to obtain a precise value for the spectral index.

3.3.2. *NGC 6334A*

The 3.5 cm map of NGC 6334A in Figure 4 clearly shows its shell-like morphology. A total flux determination from this map is uncertain because of the lack of short spacings in the observations. At 6 cm, RCM report a flux of $\sim$10 Jy for the source. We measure a shell diameter of $\sim 15''$ (0.12 pc), and a thickness of about $2''$ (0.016 pc). A gap is evident in the southern part of the shell in Figure 4. Equating the number of ionizing photons produced by an O7.5 star to the number of recombinations in the shell, we estimate the density at $n_e \sim 2 \times 10^4$ cm^{-3} and the mass of ionized gas in the shell at $M_{\rm H\,II} \sim 0.4\ M_\odot$, assuming spherical symmetry. In addition to the shell-like structure, the 3.5 cm map shows an unresolved source located near the shell center. Its position is $\alpha(2000) = 17^{\rm h}20^{\rm m}19\fs203$; $\delta(2000) = -35°54'41\farcs22$, with an error of $0\farcs03$, and its flux density is 6.1 ± 0.9 mJy. This flux density was obtained from a map made by removing short spacings below 70 kλ (equivalent to suppressing structures with angular sizes larger than about $3''$) and with uniform weight. In addition, a primary beam correction was applied using PBCOR. The infrared source IRS 19, indicated in Figure 4, lies about $6''$ southeast of the compact radio source. There are no known counterparts to the radio source. The central location of the radio source suggests that it might be associated with the star exciting the H II region. Multifrequency observations are required to investigate the nature of the radio emission.

3.3.3. *G351.02+0.65*

This source is shown in Figure 5 where our 330 MHz contour plot has been superposed on the red image of the Palomar Sky Survey. The radio morphology of G351.02+0.65 is shell-like with a large opening toward the southwest. An asymmetry is also evident in the red image of the Palomar catalog, where the source has a limb-brightened circular

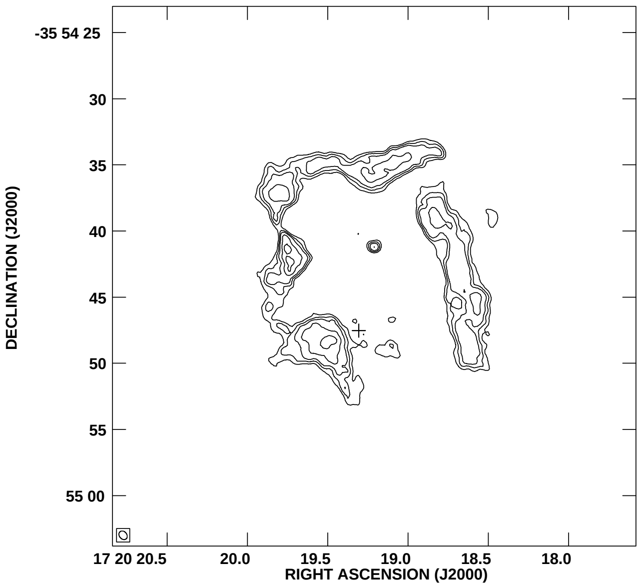

FIG. 4.—The 3.5 cm image of the H II region NGC 6334A. Contours are −4, 4, 5, 6, 8, 10 and 12 × 1.3 mJy beam^{-1}, the rms noise of the image. The compact source near the center of the nebula is proposed to trace the exciting star. There are no known counterparts to this radio source. The small cross marks the position of IRS 19, taken from 2MASS. The half-power contour of the beam (0.″72 × 0.″56; P.A. = 41°) is shown in the bottom left corner of the image.

morphology but the circle is "truncated" toward the southwest. The fact that the radio shell extends farther than the optical image suggests that the optical asymmetry arises from obscuration local to the NGC 6334 complex. In the Palomar images two bright sources are located near the shell's center; this is the visual binary system HD 319703AB. Component A, located at $\alpha(2000) = 17^{\rm h}19^{\rm m}46\overset{\rm s}{.}15$; $\delta(2000) = -36°05'52\overset{''}{.}2$, is an O7.5 III(f) star, while component B, about 13″ distant, is an O6.5 V(f) star (Chlebowski, Harnden, & Sciortino 1989). No 330 MHz emission was detected from these stars at a 3 σ level of 21 mJy. Unfortunately, this upper limit is not stringent. G351.02+0.65 was also detected at 20 cm by the NVSS (Condon et al. 1998) and at 6 cm with the VLA (archive data).

The radio shell of G351.02+0.65 is relatively extended with a diameter of about 7′, or 3.5 pc. The thickness of the shell is about 50″, or 0.4 pc. The 330 MHz flux measurement is rather uncertain due to contamination from extended emission in the region. From a map obtained using the parameter ROBUST = −5, which is equivalent to uniform weighting, we measure a flux density of 6 Jy for the shell. This, however, is probably a lower limit due to the undersampling of extended emission. The 6 cm map suffers from the same undersampling due to lack of short spacings. The shell is clearly detected at 6 cm but the flux determination is quite uncertain; a lower limit is about 4.5 Jy. From the NVSS image of G351.02+0.65 we measure a 20 cm flux of about 2 Jy. Compared with the 90 cm flux density of 6 Jy it appears that the shell's radio spectrum has a negative slope, suggesting synchrotron radiation. Further suggestion of a synchrotron origin for the radiation comes from the fact that the NVSS images show evidence for partial linear polarization of the radio emission. A linear polarization of about 4% is suggested by the observations. If the radio emission is synchrotron, G351.02+0.65 is probably a young supernova remnant. This source is not found, however, in the updated Green catalog of SNRs[2] or the pulsar catalog of Taylor, Manchester, & Lyne (1993). We caution that the uncertainties of the flux densities are large and the detection of linearly polarized radiation is marginal. Alternatively, HD 319703AB could be the ionization source of the region. Dedicated radio and/or optical observations are needed to investigate the nature of this object.

3.4. *Shell-like Compact* H II *Regions: The Age Problem*

We have described radio observations of NGC 6334 in which three radio sources present shell-like morphology. A fourth shell-like region in NGC 6334, the H II region G351.20+0.70, was mapped by Jackson & Kraemer (1999) with the VLA at 3.5 cm. In their map we measure a shell diameter of ~2.′2, or 1.1 pc, and a width of ~26″, or 0.2 pc. The diameters of the four shells in the region vary from about 3.5 to 0.12 pc, the bigger ones being located to the southwest of the complex. Of the four shells, at least three are H II regions, and two of them have central radio sources. From the values listed in Table 3 we note that the ratio of shell thickness to diameter remains relatively constant (from 0.11 to 0.18) compared with the shell diameters that vary by a factor of about 30.

Several models have been proposed to explain shell structure H II regions; these include (1) wind-driven bubbles, (2) dust cocoons, (3) champagne flows, and (4) mass-loading models. In the wind-driven bubble model the mechanical input from the stellar wind dominates the dynamics of the region and determines its evolution (Castor, McCray, & Weaver 1975; Weaver, McCray, & Castor 1977; Shull 1980). In the cocoon models a remnant shell of gas and dust is left from the process of star formation and kept from falling into the star by the stellar radiation pressure (Davidson & Harwit 1967; Kahn 1974; Cochran & Ostriker 1977; Yorke & Krugel 1977). The champagne model describes the flow produced when an expanding H II region breaks through the edge of a cloud, producing a bright rim and an evacuated cavity after the flow has emptied into the surrounding intercloud medium (Tenorio-Tagle 1979; Bedijn & Tenorio-Tagle 1981). Finally, in the mass-loading models the stellar UV radiation field and a powerful wind interact with clumpy material in the stellar neighborhood producing ultracompact H II regions of various morphologies (Dyson, Williams, & Redman 1995; Redman, Williams, & Dyson 1996). The wind-driven bubble is the more accepted model, but serious problems appear when it is applied to young, shell-like H II regions (e.g., Turner & Matthews 1984; Breitschwerdt & Kahn 1994).

Our detection of central sources associated with two young shells seems to support the wind-driven bubble model. Assuming that the central radio sources in NGC 6334E and NGC 6334A are associated with stellar winds, one can estimate the mass-loss rate $\dot{M}$, following the calculations of Panagia & Felli (1975). If we assume a wind electron temperature of $T = 10^4$ K, a wind velocity of $v_{\rm exp} = 1000$ km s^{-1}, an average ionic charge of $\bar{Z} = 1$, and a mean atomic weight per electron, $\mu = 1.2$, we derive $\dot{M} = 8.5 \times 10^{-6}\ M_\odot$ yr^{-1} for NGC 6334E, given the mea-

[2] At http://www.mrao.cam.ac.uk/surveys/snrs.

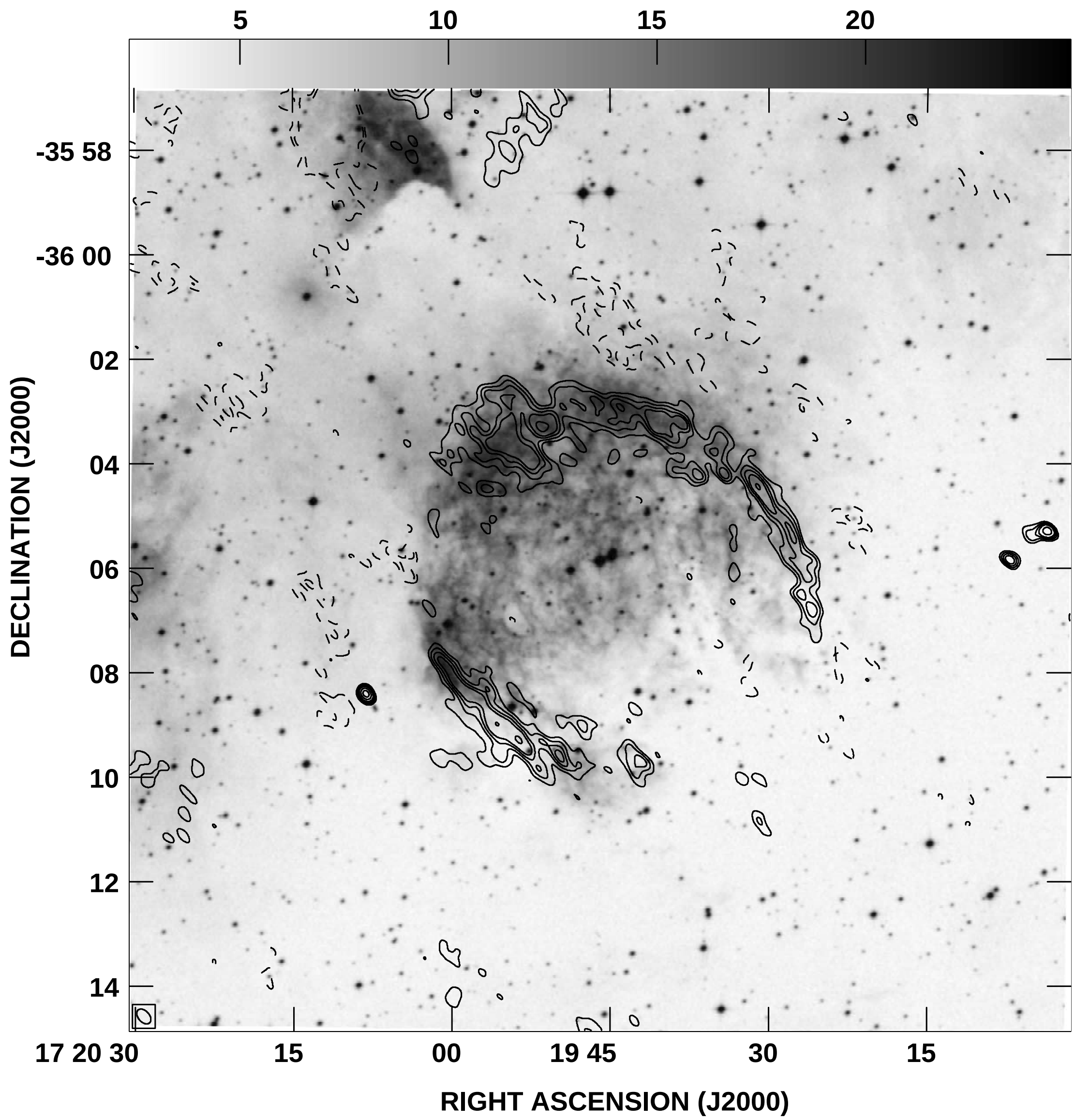

FIG. 5.—Overlay of the VLA 330 MHz image (*contours*) on the Palomar red image. The radio continuum emission generally coincides well with the edge of the nebulosity seen in the Palomar plate. Several bright sources are seen in the radio contours; they are probably extragalactic objects. The two bright stars at the center of the nebula are the binary system HD 319703AB. Contour levels for the 330 MHz continuum are −4, −3, 3, 4, 5, 6, 8, and 10 × 7 mJy beam^{-1}. The synthesized beam of the VLA image is shown in the bottom left corner.

sured flux. The corresponding mechanical luminosity would be $L_w = 2.7 \times 10^{36}$ ergs s^{-1}. Similarly for NGC 6334A, the estimated mass-loss rate is $\dot{M} = 3.0 \times 10^{-5}\ M_\odot$ yr^{-1} with a mechanical luminosity of $L_w = 9.6 \times 10^{36}$ ergs s^{-1}. Such high values of $\dot{M}$ have been measured in early-type stars with luminosities $L \sim 10^6\ L_\odot$ (e.g., Garmany & Conti 1984; Abbott, Bieging, & Churchwell 1981), but in NGC 6334E and NGC 6334A the ionization of each region implies an O7.5 ZAMS star with a corresponding luminosity of only $L \sim 8 \times 10^4\ L_\odot$. Wind velocities can be as low as ~400 km s^{-1}, which would reduce the $\dot{M}$ estimates by about 60%. Even then, given the estimated luminosity, the mass-loss rates seem to be high in these young, obscured objects. Strong stellar winds associated with NGC 6334E, NGC 6334A, and G351.20+0.70 might explain the shell-like morphology of the H II regions as resulting from a wind interaction with the ambient medium, since the mechanical input from the stellar wind will dominate the dynamics over the ionizing photons from the star (e.g., Shull 1980).

When observations of compact, shell-like H II regions are compared with the predictions of the wind-driven bubble models, several problems are apparent (e.g., Turner & Matthews 1984; Breitschwerdt & Kahn 1994). In particular, their relatively small size, the larger than expected thickness of the H II shells, and the ubiquity of these regions remain a puzzle. The small sizes observed for ultracompact, shell-like H II regions imply ages $\lesssim 500$ yr (Turner & Matthews 1984). Given the estimated wind luminosities for NGC 6334E and NGC 6334A, the models predict ages of 1000 and 200 yr, respectively, assuming an ambient density $n_{\mathrm{H_2}} = 10^3$ cm^{-3} (Shull 1980). A factor of 100 increase in the ambient density would increase the age by a factor of ~4.5. Even for the larger shell in G351.20+0.70, with a radius of about 0.55 pc, the predicted age, assuming an ambient density of 10^3 cm^{-3}

and a wind luminosity $L_w = 10^{36}$ ergs s^{-1}, is only 1.6×10^4 yr. It is unlikely that the compact H II regions are so young, because such short ages are inconsistent with the relatively large number of regions observed (Wood & Churchwell 1989a, 1989b). Furthermore, it has been noted (e.g., Redman, Williams, & Dyson 1998) that many cometary regions show shell-like morphologies when fully imaged with sensitivity to compact as well as ultracompact structures. Redman et al. (see also Turner & Matthews 1984) also note that some H II regions might be more appropriately described as "rings" rather than shells, because of the high contrast between the edge and the center. Wind-blown bubbles as young as the estimates above suggest should be expanding at velocities of hundreds of kilometers per second, while the recombination line observations of NGC 6334A indicate expansion velocities below 10 km s^{-1} (De Pree et al. 1995).

To alleviate the age problem in shell-like compact H II regions, several suggestions have been made that involve the appearance of gaps in the shells, such as we see in the three shell regions reported here. Such gaps would allow photons and the hot gas (the shocked wind layer) to escape from the cavity, thereby relieving the pressure that drives the shell expansion (e.g., Turner & Matthews 1984; Breitschwerdt & Kahn 1994). One scenario that could cause fragmentation or gaps in the shells is the evolution of a wind-driven bubble in a medium with density gradients. As the bubble expands, the density gradient might produce gaps in the shell that permit the hot gas and photons to escape, consequently reducing the expansion rate of the shell. For NGC 6334A it has been suggested that a thick molecular torus is responsible for the bipolarity of the radio lobes (Kraemer et al. 1997) as a sudden drop in density in the ambient medium would cause gaps in the shell as it expands. Franco et al. (2000) report evidence for density gradients in ultracompact H II regions that reflect density structure in the ambient gas. Numerical models of expanding H II regions (e.g., García-Segura & Franco 1996) predict instabilities that might also give rise to the "blowout" of high-pressure gas. Redman et al. (1998) have shown that mass-loading H II regions with a nonspherical distribution of mass injection can model ultracompact H II regions of various morphologies. The expansion of a wind-blown bubble in an inhomogeneous medium, however, has not yet been numerically modeled; such models would be useful to compare with the observations. In addition, high-resolution studies of the gas distribution around shell-like H II regions would also help to investigate the density structure around these objects.

4. CONCLUSIONS

Our main conclusions are the following:

1. High-sensitivity 3.5 cm VLA observations of the NGC 6334I(N) molecular core show two compact radio sources. One of them lies within 0."3 of a bright Class II methanol maser. This is the first detection of a radio continuum source in the NGC 6334I(N) region. This source is probably associated with an embedded, massive young object. If the radio emission is optically thin free-free, a B3 star would be required to provide the ionizing photons.

2. Four radio sources with shell-like morphology have been identified in NGC 6334. The shell diameters vary from ~0.12 to 3.5 pc. In two of these shell H II regions, NGC 6334E and NGC 6334A, a compact radio source was found at the shell center. These compact sources are believed to be associated with the ionizing stars, with the radio emission probably arising from ionized stellar winds. Although the wind-driven bubble is the favored model to explain the shell morphology, serious problems still exist when comparing it with observations. It is suggested that density gradients in the molecular cores could affect the evolution of the expanding bubbles by fragmenting the shells and reducing their expansion rates. Multifrequency observations of the compact sources in NGC 6334E and NGC 6334A are required to confirm their nature.

3. From the current data it is not possible to conclude whether the shell source G351.02+0.65 is an H II region or a supernova remnant. Dedicated optical and radio observations should be made of this object.

We are grateful for helpful comments by an anonymous referee, which improved the clarity of the manuscript. P. C. acknowledges support from CONACyT México. S. K. and L. F. R. acknowledge support from DGAPA, UNAM, and CONACyT, México. R. A. acknowledges support from the AMC, México. We thank S. J. Arthur for helpful discussions. This publication makes use of data products from the Two-Micron All Sky Survey, which is a joint project of the University of Massachusetts and IPAC/Caltech, funded by NASA and the NSF. The Palomar image presented in Figure 5 was obtained from the Digitized Sky Survey, which was produced at the Space Telescope Science Institute under grant NAG W-2166.

REFERENCES

Abbott, D. C., Bieging, J. H., & Churchwell, E. 1981, ApJ, 250, 645
Bachiller, R., & Cernicharo, J. 1990, A&A, 239, 276
Bedijn, P. J., & Tenorio-Tagle, G. 1981, A&A, 98, 85
Breitschwerdt, D., & Kahn, F. D. 1994, Ap&SS, 216, 297
Carral, P., Kurtz, S., Rodríguez, L. F., de Pree, C., & Hofner, P. 1997, ApJ, 486, L103
Carral, P., Kurtz, S., Rodríguez, L. F., Martí, J., Lizano, S., & Osorio, M. 1999, Rev. Mexicana Astron. Astrofis., 35, 97
Castor, J., McCray, R., & Weaver, R. 1975, ApJ, 200, L107
Caswell, J. L. 1997, MNRAS, 289, 203
Caswell, J. L., Gardner, F. F., Norris, R. P., Wellington, K. J., McCutcheon, W. H., & Peng, R. S. 1993, MNRAS, 260, 425
Cheung, L., Frogel, J. A., Hauser, M. G., & Gezari, D. Y. 1978, ApJ, 226, L149
Chlebowski, T., Harnden, F. R., & Sciortino, S. 1989, ApJ, 341, 427
Cochran, W. D., & Ostriker, J. P. 1977, ApJ, 211, 392
Condon, J. J., Cotton, W. D., Greisen, E. W., Yin, Q. F., Perley, R. A., Taylor, G. B., & Broderick, J. J. 1998, AJ, 115, 1693
Davidson, K., & Harwit, M. 1967, ApJ, 148, 443
Davis, C. J., & Eisloeffel, J. 1995, A&A, 300, 851
De Pree, C. G., Rodríguez, L. F., Dickel, H. R., & Goss, W. M. 1995, ApJ, 447, 220
Dickel, H. R., Dickel, J. R., & Wilson, W. J. 1977, ApJ, 217, 56
Dyson, J. E., Williams, R. J. R., & Redman, M. P. 1995, MNRAS, 277, 700
Forster, J. R., & Caswell, J. L. 1989, A&A, 213, 339
Forster, J. R., Whiteoak, F. F., Gardner, F. F., Peters, W. L., & Kuiper, T. B. H. 1987, Proc. Astron. Soc. Australia, 7, 2
Franco, J., Kurtz, S., Hofner, P., Testi, L., García-Segura, G., & Martos, M. 2000, ApJ, 542, L143
García-Segura, G., & Franco, J. 1996, ApJ, 469, 171
Garmany, C. D., & Conti, P. S. 1984, ApJ, 284, 705
Gaume, R. A., & Mutel, R. L. 1987, ApJS, 65, 193
Gezari, D. Y. 1982, ApJ, 259, L29
Harvey, P. M., & Gatley, I. 1983, ApJ, 269, 613
Harvey, P. M., Hyland, A. R., & Straw, S. M. 1987, ApJ, 317, 173
Jackson, J. M., & Kraemer, K. E. 1999, ApJ, 512, 260
Kahn, F. 1974, A&A, 37, 149
Kraemer, K. E., & Jackson, J. M. 1995, ApJ, 439, L9

Kraemer, K. E., & Jackson, J. M. 1999, ApJS, 124, 439
Kraemer, K. E., Jackson, J. M., Paglione, T. A. D., & Bolatto, A. D. 1997, ApJ, 478, 614
Kogan, L., & Slysh, V. 1998, ApJ, 497, 800
Kuiper, T. B. H., Peters, W. L., III, Forster, J. R., Gardner, F. F., & Whiteoak, J. B. 1995, ApJ, 446, 692
Loughran, L., McBreen, B., Fazio, G. G., Rengarajan, T. N., Maxson, C. W., Serio, S., Sciortino, S., & Ray, T. P. 1986, ApJ, 303, 629
Mangum, J. G., & Wootten, A. 1993, ApJS, 89, 123
McBreen, B., Fazio, G. G., Stier, M., & Wright, E. L. 1979, ApJ, 232, L183
McCutcheon, W. H., Sandell, G., Matthews, H. E., Kuiper, T. B. H., Danchi, W. C., & Sato, T. 2000, MNRAS, 316, 152
Megeath, S. T., & Tieftrunk, A. R. 1999, ApJ, 526, L113
Menten, K. M., & Bartla, W. 1989, ApJ, 341, 839
Miller, G. E., & Scalo, J. M. 1979, ApJS, 41, 513
Moran, J. M., & Rodríguez, L. F. 1980, ApJ, 236, L159
Moran, J. M., Rodríguez, L. F., Greene, B., & Backer, D. C. 1990, ApJ, 348, 147
Neckel, T. 1978, A&A, 69, 51
Norris, R. P., Whiteoak, J. B., Caswell, J. L., Wieringa, M. H., & Gough, R. G. 1993, ApJ, 412, 222
Panagia, N., & Felli, M. 1975, A&A, 39, 1
Persi, P., Roth, M., Tapia, M., Marenzi, A. R., Felli, M., Testi, L., & Ferrari-Toniolo, M. 1996, A&A, 307, 591
Redman, M. P., Williams, R. J. R., & Dyson, J. E. 1996, MNRAS, 280, 661
———. 1998, MNRAS, 298, 33
Rodríguez, L. F., Cantó, J., & Moran, J. M. 1982, ApJ, 255, 103 (RCM)
———. 1988, ApJ, 333, 801
Sandell, G. 2000, A&A, 358, 242
Shull, M. J. 1980, ApJ, 238, 860
Tapia, M., Persi, P., & Roth, M. 1996, A&A, 316, 102 (TPR)
Taylor, J. H., Manchester, R. N., & Lyne, A. G. 1993, ApJS, 88, 529
Tenorio-Tagle, G. 1979, A&A, 71, 59
Turner, B. E., & Matthews, H. E. 1984, ApJ, 277, 164
Weaver, R., McCray, R., & Castor, J. 1977, ApJ, 218, 377
Walsh, A. J., Burton, M. G., Hyland, A. R., & Robinson, G. 1998, MNRAS, 301, 640
Wood, D. O. S., & Churchwell, E. 1989a, ApJS, 69, 831
———. 1989b, ApJ, 340, 265
Yorke, H. W., & Krugel, E. 1977, A&A, 54, 183